HHS Public Access

Author manuscript

J Biomed Mater Res A. Author manuscript; available in PMC 2021 February 01.

Published in final edited form as:

J Biomed Mater Res A. 2020 February ; 108(2): 246–253. doi:10.1002/jbm.a.36811.

Pectin Biopolymer Mechanics and Microstructure Associated with Polysaccharide Phase Transitions

Aidan Pierce[1], **Yifan Zheng**[1], **Willi L. Wagner**[1,2], **Henrik V. Scheller**[3], **Debra Mohnen**[4], **Akira Tsuda**[5], **Maximilian Ackermann**[6], **Steven J. Mentzer**[1,*]

[1]Laboratory of Adaptive and Regenerative Biology, Brigham & Women's Hospital, Harvard Medical School, Boston MA

[2]Department of Diagnostic and Interventional Radiology, Translational Lung Research Center, University of Heidelberg, Heidelberg, Germany

[3]Joint BioEnergy Institute, Emeryville CA and the Environmental Genomics and Systems Biology Division, Lawrence Berkeley National Laboratory, Berkeley, CA

[4]Complex Carbohydrate Research Center and Department of Biochemistry and Molecular Biology, University of Georgia, Athens, GA

[5]Molecular and Integrative Physiological Sciences, Harvard School of Public Health, Boston, MA

[6]Institute of Functional and Clinical Anatomy, University Medical Center of the Johannes Gutenberg-University, Mainz, Germany

Abstract

Polysaccharide polymers like pectin can demonstrate striking and reversible changes in their physical properties depending upon relatively small changes in water content. Recent interest in using pectin polysaccharides as mesothelial sealants suggests that water content, rather than nonphysiologic changes in temperature, may be a practical approach to optimize the physical properties of the pectin biopolymers. Here, we used humidified environments to manipulate the water content of dispersed solution of pectins with a high degree of methyl esterification (high-methoxyl pectin; HMP). The gel phase transition was identified by a nonlinear increase in compression resistance at a water content of 50% (w/w). The gel phase was associated with a punched-out fracture pattern and SEM images that revealed a cribiform (Swiss cheese-like) pectin microstructure. The glass phase transition was identified by a marked increase in resilience and stiffness. The glass phase was associated with a star-burst fracture pattern and SEM images that demonstrated a homogeneous pectin microstructure. In contrast, the burst strength of the pectin films was largely independent of water content over a range from 5% to 30% (w/w). These observations indicate the potential to use water content in the selective regulation of the physical properties of HMP biopolymers.

*Corresponding author: smentzer@bwh.harvard.edu (SJM).

The authors confirm that there are no known conflicts of interest associated with this publication and there has been no significant financial support for this work that could have influenced its outcome.

Introduction

A variety of polysaccharide polymers have been used in tissue engineering applications including alginate,[1] agarose,[2] cellulose,[3] chitin[4] and pectin[5]. Pectin is a particularly versatile polysaccharide because of its chemical and structural features.[6,7] Chemically, a unique characteristic of pectin is its high content of partially esterified linear chains of (1,4)-alpha-D-galacturonic acid residues that are resistant to acid environments and proteolytic enzymes.[8–10] Pectin is a heteropolysaccharide that is an important component of the middle lamella of most plants.[11] In addition to the linear chains of galacturonic acid residues, known as homogalacturonan or polygalacturonan, pectin is composed of highly branched pectic domains known as rhamnogalacturonan I (RGI), which have a complex composition that differs between plant species[5]. An additional branched pectin domain, RGII, also exists in plant cell walls but is present in lower amounts and is more conserved across different species and cell types.[12] The physical interaction of these branched domains, and in particular RGI, has been suggested as an explanation for pectin's adhesivity to the mesothelial glycocalyx of visceral organs[5,13,14], although the specific role(s) of the homogalacturonan versus branched domains in the adhesivity of pectin to the mesothelial matrix remains to be determined. It is this distinctive adhesive property that has led to pectin's proposed use as a mesothelial sealant.[5,13,14]

An intriguing feature of polysaccharide polymers are their adjustable physical properties; a phenomenon typically associated with changes in temperature and water content.[15,16] Although temperature manipulations are limited in biomedical applications, polysaccharide polymers like pectin can demonstrate striking and reversible changes in their physical properties in the presence of even trace amounts of water.[17] The loss of water alone from a dispersed solution of pectins with a high degree of methyl esterification (so-called high-methoxyl pectins) can lead to the initial polymerization of the pectin.[18] This so-called "gel transition" is associated with a discrete change in the physical properties of the pectin from a viscous liquid to a soft and rubbery gel.[19,20] The ongoing loss of water from the pectin gel leads to a second discrete step, so-called "glass transition," associated with a change in the physical properties of the pectin from soft and rubbery to hard and brittle. Although the emergence of these physical properties suggests discrete stages in pectin organization, the microstructural implications of these phase transitions remain unclear.[21–23]

In this report, we studied tunable mechanical and microstructural properties of high-methoxyl pectin (HMP) films as a function of water content alone. Using controlled humidity environments and film properties relevant to biomedical applications, we demonstrated the practical features of the phase transitions commonly associated with pectin polysaccharides.

Methods

Pectin. Pectin.

The citrus pectins were obtained from a commercial source (Cargill, Minneapolis, MN, USA) with a glycosyl residue content of 78–86% mole % galacturonic acid, 2–3% rhamnose, 9–14% galactose and 0.5–5% arabinose based on gas chromatography–mass

spectrometry of trimethylsilyl derivatives[24] and a 77–85% homogalacturonan and 16–23% RGI content. The proportion of galacturonic acid residues in the methyl ester form determined the degree of methoxylation. High-methoxyl pectins (HMP) were defined as those pectin polymers with a greater than 50% degree of methoxylation (Mean=67±8%). The pectin powder was stored at 20% relative humidity and 25°C.

Pectin dissolution in water.

The pectin powder was dissolved at 25°C by a step-wise increase in added water to avoid undissolved powder to 3% (w/w);[25] exogenous heat was not used. Swelling and softening of the particles was followed by fluidization and dissolution.[26] The complete dissolution of the pectin was achieved by a high-shear 10,000 rpm rotor-stator mixer (L5M-A, Silverson, East Longmeadow, MA USA). Plateau viscosity was monitored using digital tachometer and ammeter (DataLogger, Silverson). The dissolved pectin was poured into a standard mold for further studies.

Humidification chamber.

A custom designed 5.7-liter translucent polycarbonate humidification chamber constructed to be air-tight when sealed, as well as compatible with the materials analyzer (TA-XT plus, Stable Micro Systems) for serial measurements, was used. Humidification was produced by an ultrasonic humidifier or manual aerosol device. The chamber was monitored by wireless (bluetooth) hygrometer and thermometer sensors (Inkbird, Shenzhen, PRC). The data recording device was maintained within the humidification chamber throughout each experiment.

Compression and decompression.

Compression testing was performed to determine the behavior of the films under a compressive load. After calibration of the 5 kg load cell (TA-XT plus, Stable Micro Systems) a 25 mm diameter acrylic disc was mounted to the crosshead over the center of the pectin polymer. The disc contacted the film at a test speed of 1 mm/sec and probed to a depth of 50% of the standardized film thickness (calibrated by AT-XT plus) to record the peak or maximum force on compression (positive deflection). The area under the positive curve was defined as the work of compression. The disc was then withdrawn at a test speed of 1 mm/sec to record the force required to withdraw the disc from the pectin (negative deflection). Data were acquired at 500 points per second

Resilience and stiffness.

Resilience testing was performed to determine the elastic energy absorbed by the pectin biopolymers; that is, the area under the elastic portion of the stress-strain curve. Resilience, stiffness and springiness were measured using an TA-XT plus (Stable Micro Systems). After calibration of the 5 kg load cell, a 5 mm spherical probe descended at a test speed of 1 mm/sec (1 gm trigger force) to a limit of 85% strain and was withdrawn at the identical speed. The ratio of the area under the force curve during compression (Area 1) and withdrawal (Area 2) was defined as resilience (R=Area 2/Area 1). Stiffness was defined as the slope of the linear portion of the compression curve.

Fracture mechanics.

To determine the pattern and topology of the fracture, the biopolymers were subjected to a controlled uniaxial load normal to the plane of the polymer film. A 5 mm stainless steel spherical probe was mounted to a 5 kg load cell and positioned centrally over the biopolymer. The probe compressed the biopolymers at a test speed of 0.5 mm/sec until fracture. The fracture force and distance were recorded at 500 pps.

Scanning electron microscopy.

After coating with 20–25 A gold in an argon atmosphere, the pectin films were imaged using a Philips XL30 ESEM scanning electron microscope (Philips, Eindhoven, Netherlands) at 15 Kev and 21 μA. Stereo pair images were obtained using a tilt angle difference of 6° on a eucentric sample holder using standardized automation.

Statistical analysis.

The statistical analysis was based on a minimum of 100 films derived from at least three different pectin batches. The unpaired Student's t test for samples of unequal variances was used to calculate statistical significance. The data were expressed as mean ± one standard deviation. The significance level for the sample distribution was defined as $p<.01$. The coefficient of determination or R^2 was determined for each test. Residual plots were assessed for systematic error.

Results

Pectin film preparation.

With the appropriate intrinsic conditions,[27] evaporation alone is sufficient for a distinct change in physical properties of high-methoxyl pectin (HMP).[28] HMP films (2% to 4% w/w in water) were prepared using a high-shear mixer (Figure 1A). The HMP films were cured in a 20% relative humidity environment. In this environment, there was a subjective change in the physical properties of the films at 12 hours and 24 hours corresponding to classic definitions of gel and glass transitions[29] (Figure 1B). To provide an empirical measure of gelation, a flat cylinder probe was programmed to penetrate to a depth of 50% of the film thickness (Figure 1C) with measurement of both compression and withdrawal forces (Figure 1D). The compression test demonstrated a marked increase in required compression force at 12 hours (Figure 1E). Similarly, the withdrawal of the probe, corresponding to the stickiness and cohesion of the films, also demonstrated a marked increase after 12 hours (Figure 1F).

Pectin film resilience.

To assess the response to physical deformation, we measured the effect of water content on film resilience and stiffness. The films were probed with a 5 mm spherical stainless-steel probe to 70% estimated strain (Figure 2A). Resilience was calculated as the ratio between the absorbed energy during film deformation and the released energy during unloading (Figure 2B). The resilience curves demonstrated progressive displacement with increasing water content (Figure 2C). The corresponding resilience curves showed a decrease in resilience (Figure 2D; $R^2=0.974$) and increase in deformation distance (Figure 2E;

R^2=0.859) with increased water content. Similarly, the measured polymer stiffness decreased with increased water content (Figure 2F; R^2=0.999).

Glass transition.

To assess film burst strength, we assessed the effect of water content on film burst force and fracture pattern. The films were probed at a controlled rate (2 mm/sec) until film rupture; the required force and distance were recorded (Figure 3A). The burst testing demonstrated comparable burst strength, but increasing extensibility, with increased water content (Figure 3B). Despite occasional outliers likely related to film preparation defects, the trends of preserved burst strength were consistent (Figure 3C). In contrast, extensibility increased with increasing water content (Figure 3D). Finally, the deformation-induced fracture pattern provided a practical definition of the glass transition. Water content greater than 20% (w/w) was associated with the ‘punched-out’ fracture pattern representative of gel films (Figure 3E). In contrast, films with water content less than 5% (w/w) demonstrated the ‘star-burst’ fracture pattern characteristic of glass films (Figure 3F).

Fracture patterns.

To assess the microstructure associated with gel and glass transitions, we examined the fracture patterns of films using scanning electron microscopy (SEM). The fracture patterns of films with water content greater than 20% (w/w) demonstrated a simple line fracture or, more commonly, a simple ‘punched-out’ hole in the film reflecting the dimensions of the spherical probe (Figure 4A). An interesting feature of these films was the presence of amorphous pools between cribiform (Swiss cheese-like) bands of polymerized pectin networks (Figure 4B–D). In contrast, the fracture patterns of pectin films with water content less than 5% (w/w) demonstrated in a ‘star-burst’ pattern with distinctive angles (Figure 5A–B). Distinct from the gel-associated films, the fracture interface demonstrated continuous polymerized networks (Figure 5C–D).

Discussion

In this report, we studied the tunable mechanical and microstructural properties of high-methoxyl pectin (HMP) films as a function of water content alone. Using controlled humidity environments, we demonstrated several practical features of HMP phase transitions. First, the gel phase transition was identified by a nonlinear increase in compression resistance at a water content of 50% (w/w). The gel phase was associated with a punched-out fracture pattern and SEM images that revealed a cribiform (Swiss cheese-like) pectin microstructure. Second, the glass phase transition was identified by a marked increase in resilience and stiffness. The glass phase was associated with a star-burst fracture pattern and SEM images that demonstrated an apparent homogeneous pectin microstructure. Third, the burst strength of the pectin films was largely independent of water content over a range from 5% to 35% (w/w). Together, these observations illustrate the dynamic role of water content in regulating many—but not all—of the physical properties of pectin biopolymers.

The conventional interpretation of gel and glass transition points is that these state transitions reflect discrete stages in the self-assembly of 3-dimensional pectin networks. Although the intermediate energy landscape remains unclear,[30–32] the liquid phase appears to be a high energy state associated with high configurational entropy and significant opportunity for molecular oscillation. The progressive loss of water is associated with a loss of energy and lower configurational entropy—leading to an initial stage in pectin self-assembly and the solid-like properties characteristic of gels.[33–35] The ongoing loss of water leads to a lower energy state that further limits intermolecular interactions. The apparent homogeneous polymerization of the pectin network ultimately produces physical properties described as hard and glass-like.[36,37]

The practical implications of these phase transitions are relevant to biomedical applications. For example, the ability to recover from large elastic strains during deformation is a crucial feature of pectin's functional utility as a mesothelial sealant.[14] The mesothelium, the surface layer of internal organs, is associated with extraordinary stresses during normal organ function; these stresses include the movement associated with the beating heart, ventilating lung and peristaltic bowel. To assess pectin's capacity to adapt to these changing conditions, we used the measure of resilience. Resilience, typically calculated as the area under the linear portion of the stress-strain curve, reflects the ability of a material to absorb energy when deformed and release energy when unloaded. Here, we found that resilience correlated with the density of the three-dimensional network; the near-homogenous polymer in the glass phase was linked to greater resilience.

An interesting observation was the relatively preserved burst strength of the pectin films at broad range of water content; that is, the pectin films' burst strength was largely independent of the density of pectin polymer association. This observation suggests that even the cribiform 3-dimensional pectin networks—at least in high-methoxyl pectins—provide substantial structural integrity. Presumably, the structural properties of these films reflect stabilization by the pectin macromolecules and the hydrogen and hydrophobic bonding of the water-polysaccharide system.[18,38]

A second interesting observation was the unique fracture patterns produced by glass phase pectin films. The topography of the fracture patterns (fractography), a widely applied approach in materials sciences,[39] has been used to characterize features of the material microstructure. Here, fracture mechanics not only identified the glass-transition point, but also demonstrated fractures distinct from inorganic glass fracture patterns.[40] The glass phase fracture produced a radiating pattern with a characteristic angular geometry. Notably, these fracture patterns did not display the secondary features (e.g. mirror, mist, hackle) seen in inorganic glass and appear to reflect distinctive features of pectin microstructure.

Finally, the present study, influenced by previous observations of mesothelial adhesion,[5,13] was restricted to high-methoxyl citrus pectin. Other naturally-occurring pectin variants, such as potato- or soybean-derived pectins, may provide distinctive physical properties; however, their potential utility as mesothelial sealants have yet to be demonstrated. Similarly, the use of composite materials, such as nanocellulose,[41] may modify the physical properties and expand the practical use of pectin films *in vivo*. We anticipate that pectin variants and

composite films will provide useful insights into the mechanical and microstructural properties of pectin biopolymers.

Acknowledgements

The authors would like to acknowledge the support of Gaert Maesmans, Piet Bogaert, Christoph Peters and Ivo Kohls of the Cargill Corporation.

Supported in part by NIH Grant HL94567, HL134229, HL007734, CA009535, ES000002 and the German Research Foundation (SFB1066). HSV was supported by Contract DEAC0205CH11231 between Lawrence Berkeley National Laboratory and the U.S. Department of Energy

Abbreviations:

HMP	high-methoxyl pectin
LMP	low-methoxyl pectin
SEM	scanning electron microscopy
Wc	water content

References

1. Shachar M, Tsur-Gang O, Dvir T, Leor J, Cohen S. The effect of immobilized RGD peptide in alginate scaffolds on cardiac tissue engineering. Acta Biomaterialia 2011;7(1):152–162. [PubMed: 20688198]
2. Khanarian NT, Haney NM, Burga RA, Lu HH. A functional agarose-hydroxyapatite scaffold for osteochondral interface regeneration. Biomaterials 2012;33(21):5247–5258. [PubMed: 22531222]
3. Pooyan P, Tannenbaum R, Garmestani H. Mechanical behavior of a cellulose-reinforced scaffold in vascular tissue engineering. J Mech Behav Biomed Mater 2012;7:50–59. [PubMed: 22340684]
4. Kumar PTS, Srinivasan S, Lakshmanan V-K, Tamura H, Nair SV, Jayakumar R. beta-Chitin hydrogel/nano hydroxyapatite composite scaffolds for tissue engineering applications. Carbohydr. Polym 2011;85(3):584–591.
5. Servais AB, Kienzle A, Valenzuela CD, Ysasi AB, Wagner WL, Tsuda A, Ackermann M, Mentzer SJ. Structural heteropolysaccharide adhesion to the glycocalyx of visceral mesothelium. Tissue Eng Part A 2018;24:199–206. [PubMed: 28467734]
6. Atmodjo MA, Hao ZY, Mohnen D. Evolving Views of Pectin Biosynthesis In: Merchant SS, editor. Annual Review of Plant Biology, Vol 64; 2013 p 747–+.
7. Coimbra P, Ferreira P, de Sousa HC, Batista P, Rodrigues MA, Corriea IJ, Gil MH. Preparation and chemical and biological characterization of a pectin/chitosan polyelectrolyte complex scaffold for possible bone tissue engineering applications. Int. J. Biol. Macromol 2011;48(1):112–118. [PubMed: 20955729]
8. Mohnen D Pectin structure and biosynthesis. Curr. Opin. Plant Biol 2008;11(3):266–277. [PubMed: 18486536]
9. Monsoor MA, Kalapathy U, Proctor A. Determination of polygalacturonic acid content in pectin extracts by diffuse reflectance Fourier transform infrared spectroscopy. Food Chem. 2001;74(2):233–238.
10. Nunes C, Silva L, Fernandes AP, Guine RPF, Domingues MRM, Coimbra MA. Occurrence of cellobiose residues directly linked to galacturonic acid in pectic polysaccharides. Carbohydr. Polym 2012;87(1):620–626.
11. Scheller HV, Jensen JK, Sorensen SO, Harholt J, Geshi N. Biosynthesis of pectin. Physiol. Plant 2007;129(2):283–295.

12. Bar-Peled M, Urbanowicz BR, O'Neill MA. The synthesis and origin of the pectic polysaccharide rhamnogalacturonan II - insights from nucleotide sugar formation and diversity. Frontiers in Plant Science 2012;3.
13. Servais AB, Kienzle A, Ysasi AB, Valenzuela CD, Wagner WL, Tsuda A, Ackermann M, Mentzer SJ. Structural heteropolysaccharides as air-tight sealants of the human pleura. J. Biol. Mat. Res 2018;107:799–806.
14. Servais AB, Valenzuela CD, Kienzle A, Ysasi AB, Wagner W, Tsuda A, Ackermann M, Mentzer SJ. Functional mechanics of a pectin-based pleural sealant after lung injury. Tissue Eng Part A 2018;24:695–702. [PubMed: 28920559]
15. Cavallaro G, Lazzara G, Milioto S. Dispersions of nanoclays of different shapes into aqueous and solid biopolymeric matrices. Extended physicochemical study. Langmuir 2011;27(3):1158–1167. [PubMed: 21188987]
16. Cavallaro G, Donato DI, Lazzara G, Milioto S. Films of halloysite nanotubes sandwiched between two layers of biopolymer: From the morphology to the dielectric, thermal, transparency, and wettability properties. J. Phys. Chem. C 2011;115(42):20491–20498.
17. Zheng Y, Pierce A, Wagner WL, Scheller HV, Mohnen D, Tsuda A, Ackermann M, Mentzer SJ. Analysis of pectin biopolymer phase states using acoustic emissions. Carbohydr. Polym 2019;In press.
18. Iijima M, Nakamura K, Hatakeyama T, Hatakeyama H. Phase transition of pectin with sorbed water. Carbohydr. Polym 2000;41(1):101–106.
19. Lofgren C, Guillotin S, Hermansson AM. Microstructure and kinetic rheological behavior of amidated and nonamidated LM pectin gels. Biomacromolecules 2006;7(1):114–121. [PubMed: 16398505]
20. Alba K, Kasapis S, Kontogiorgos V. Influence of pH on mechanical relaxations in high solids LM-pectin preparations. Carbohydr. Polym 2015;127:182–188. [PubMed: 25965472]
21. Al-Ruqaie IM, Kasapis S, Richardson RK, Mitchell G. The glass transition zone in high solids pectin and gellan preparations. Polymer 1997;38(22):5685–5694.
22. Einhorn-Stoll U, Kunzek H. The influence of the storage conditions heat and humidity on conformation, state transitions and degradation behaviour of dried pectins. Food Hydrocoll. 2009;23(3):856–866.
23. Lara-Espinoza C, Carvajal-Millan E, Balandran-Quintana R, Lopez-Franco Y, Rascon-Chu A. Pectin and pectin-based composite materials: Beyond food texture. Molecules 2018;23(4):35.
24. Biswal AK, Tan L, Atmodjo MA, DeMartini J, Gelineo-Albersheim I, Hunt K, Black IM, Mohanty SS, Ryno D, Wyman CE and others. Comparison of four glycosyl residue composition methods for effectiveness in detecting sugars from cell walls of dicot and grass tissues. Biotechnol. Biofuels 2017;10.
25. Panchev IN, Slavov A, Nikolova K, Kovacheva D. On the water-sorption properties of pectin. Food Hydrocoll. 2010;24(8):763–769.
26. Furmaniak S, Terzyk AP, Gauden PA. The general mechanism of water sorption on foodstuffs - Importance of the multitemperature fitting of data and the hierarchy of models. J. Food Eng 2007;82(4):528–535.
27. Lofgren C, Walkenstrom P, Hermansson AM. Microstructure and rheological behavior of pure and mixed pectin gels. Biomacromolecules 2002;3(6):1144–1153. [PubMed: 12425650]
28. Sriamornsak P. Application of pectin in oral drug delivery. Expert Opin. Drug Deliv 2011;8(8):1009–1023. [PubMed: 21564000]
29. Hermans PH. Gels. In: Kruyt HR, editor. Colloid Science; 1949.
30. Braun O, Hanke A, Seifert U. Probing molecular free energy landscapes by periodic loading. Phys. Rev. Lett 2004;93(15).
31. Morrow BH, Payne GF, Shen J. pH-Responsive Self-Assembly of Polysaccharide through a Rugged Energy Landscape. J. Am. Chem. Soc 2015;137(40):13024–13030. [PubMed: 26383701]
32. Khatri BS, Kawakami M, Byrne K, Smith DA, McLeish TCB. Entropy and barrier-controlled fluctuations determine conformational viscoelasticity of single biomolecules. Biophys. J 2007;92(6):1825–1835. [PubMed: 17158578]
33. Rinaudo M. Gelation of Polysaccharides. J. Intel. Mat. Syst. Str 1993;4(2):210–215.

34. Djabourov M. Gelation - a review. Polym. Int 1991;25(3):135–143.
35. Ross-Murphy SB. Physical gelation of biopolymers. ACS Symp. Ser 1992;489:204–216.
36. Rolin C, Nielsen BU, Glahn P-E. Pectin In: Dumitriu S, editor. Polysaccharides: Structural Diversity and Functional Versatility: CRC Press; 2004.
37. Einhorn-Stoll U. Pectin-water interactions in foods - From powder to gel. Food Hydrocoll. 2018;78:109–119.
38. Thakur BR, Singh RK, Handa AK. Chemistry and uses of pectin - A review. Crit. Rev. Food Sci. Nutr 1997;37(1):47–73. [PubMed: 9067088]
39. Hull D. Fractography: Observing, Measuring and Interpreting Fracture Surface Topography. Cambridge: Cambridge University Press; 1999 366 p.
40. Bradt RC, Tressler RE. Fractography of Glass: Springer; 1994.
41. Chaichi M, Hashemi M, Badii F, Mohammadi A. Preparation and characterization of a novel bionanocomposite edible film based on pectin and crystalline nanocellulose. Carbohydr. Polym 2017;157:167–175. [PubMed: 27987882]

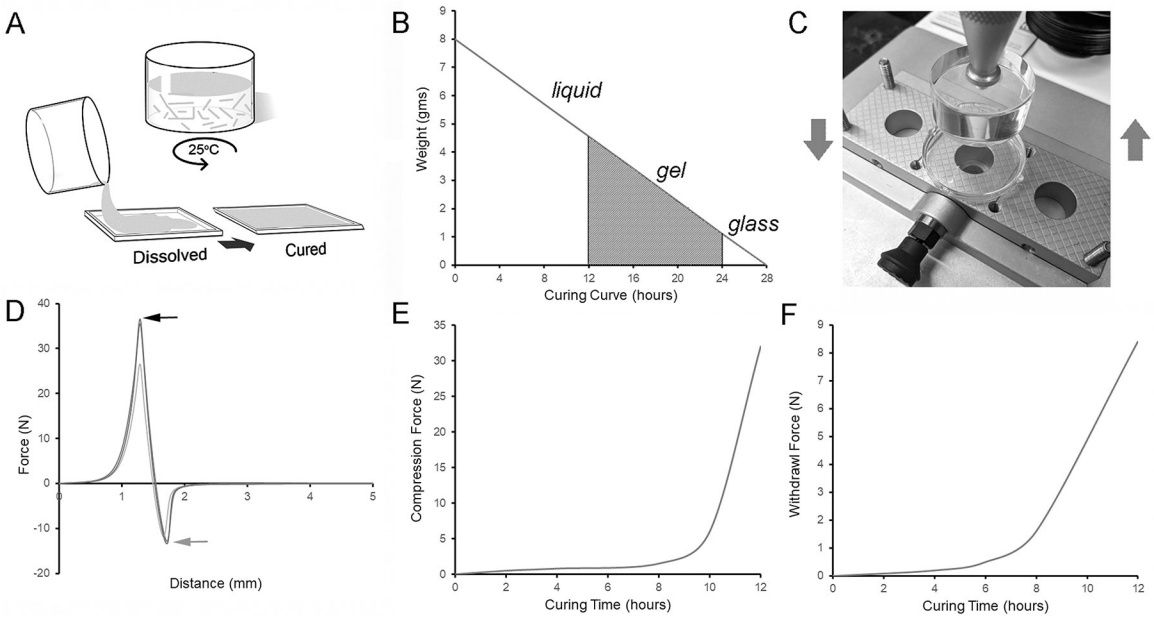

Figure 1.

Preparation of pectin films. A) Pectin solutions (3–4% w/w) were created by mixing pectin powder in deionized water using a high-shear mixer (see Methods) at room temperature. B) The dispersed solutions were cured in a 20% relative humidity environment with progressive evaporation of water. C) The pectin solutions were tested for evidence of polymerization at various times in the curing process. A load cell, mounted with a cylindrical acrylic probe, was used to identify the initial phase of phase of polymerization. D) The force required to compress the pectin solution to 50% its baseline thickness (black arrow) and withdraw probe (gray arrow) were recorded. E-F) The force required to compress and withdraw the probe were significantly increased at 12 hours.

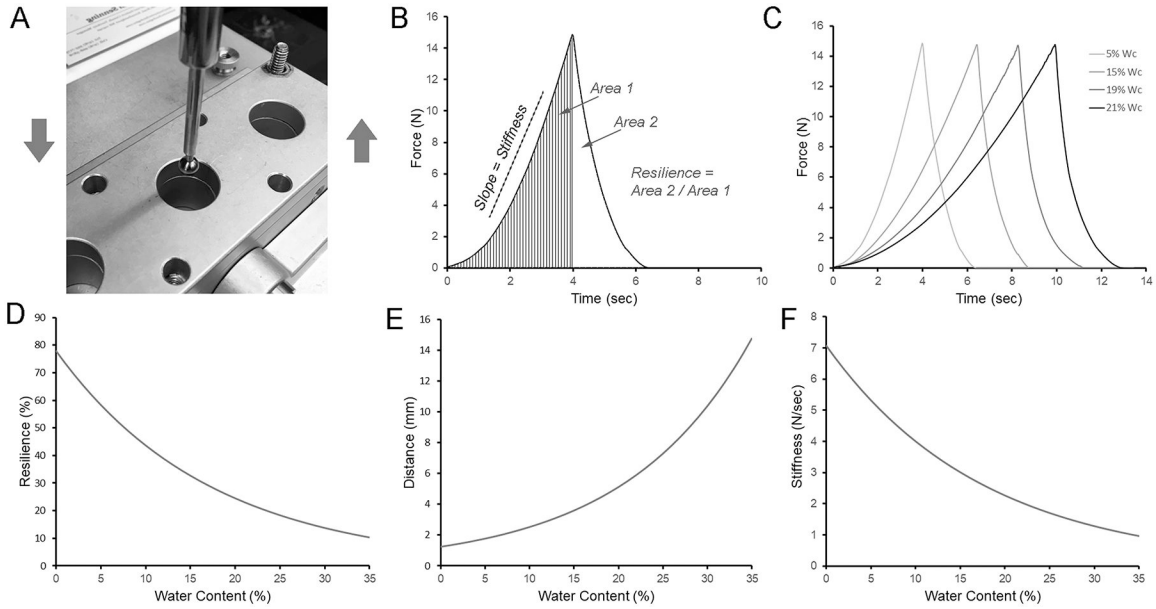

Figure 2.

Resilience and stiffness of pectin films. A) A 5 mm stainless steel sphere was used to probe the curing films to 70% estimated strain. B) The resilience was calculated as the ratio between absorbed energy during elastic deformation (Area 1) and the released energy (Area 2) upon unloading. C) Characteristic resilience curves at various stages of curing were calculated as the percent (w/w) water content. D) Resilience declined with increasing water content (curve fit, R^2=0.974). E) The distance the probe traveled to achieve 70% estimated strain increased with increased water content (R^2=0.859). F) Stiffness, reflecting the slope during loading, decreased with increasing water content (R^2=0.999).

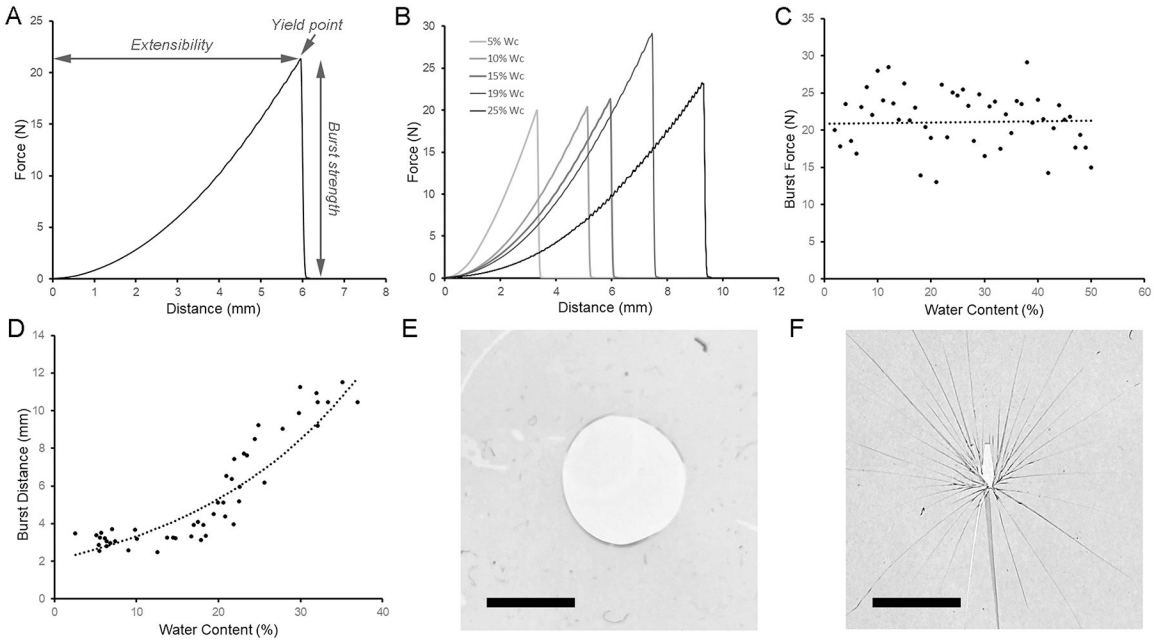

Figure 3.

Burst strength and fracture mechanics of pectin films. A) Using a spherical stainless steel probe (5mm), the pectin films were loaded (2 mm/sec) until fracture. The peak force was recorded as burst strength. The distance the probe traveled was defined as extensibility. B) Characteristic burst strength curves shown at a range of water contents. C) The burst strength was relatively independent of water content up to 30% (R^2=0.528). D) In contrast, the force-displacement (extensibility) increased with water content (R^2=0.812. Notably, the fracture patterns differed significantly between gel and glass films. E) Representative 'punched-out' fracture pattern of a film with 20% water content. F) Representative 'star burst' fracture pattern of a films with 5% water content. Bar=3mm.

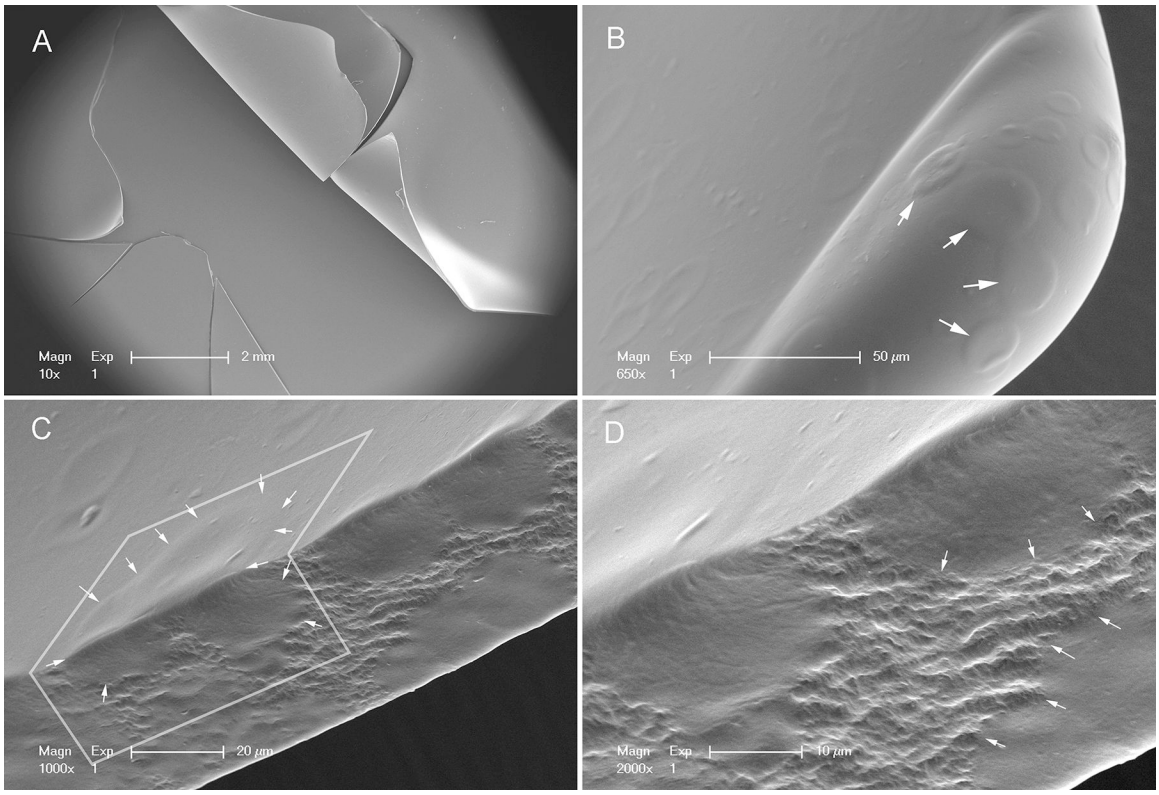

Figure 4.

Scanning electron microscopy of a film with 25% water content. A) The 'punched-out' fracture pattern reflected the diameter of the 5mm spherical probe. B) The surface of the films demonstrated circular surface irregularites (arrows). C) The interface of the fractures demonstrated that the surface irregularities corresponded to amorphous pools in the film (arrows). D) Higher resolution demonstrates the pectin network between the amorphous pools (arrows).

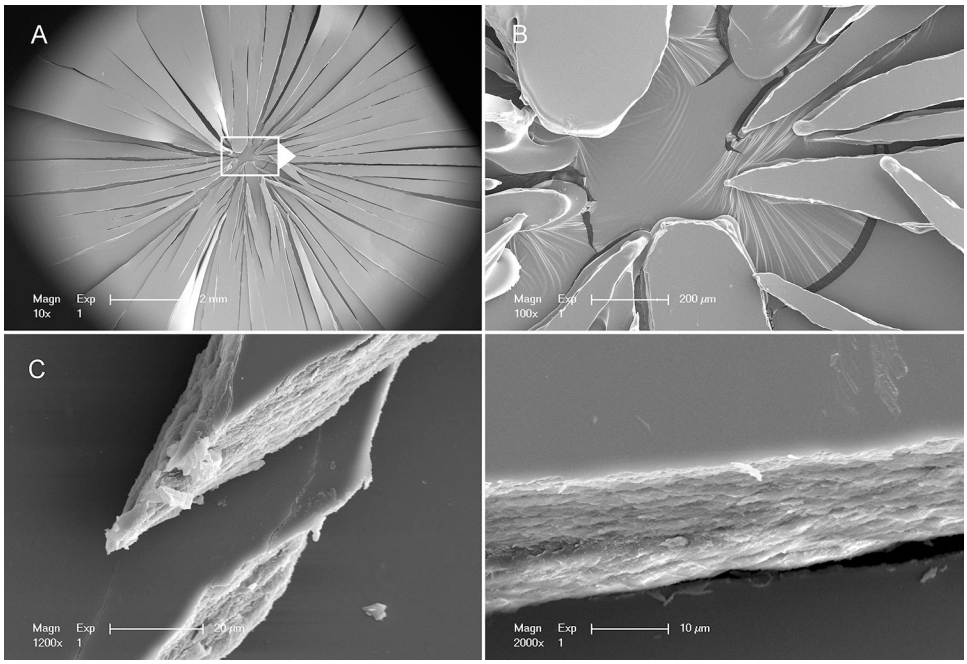

Figure 5.

Scanning electron microscopy of a film with 5% water content. A,B) The ‘star-burst’ fracture pattern radiated from the force center of the 5 mm spherical probe. C) The interface of the fractures demonstrated a dense pectin microstructure. D) Higher resolution demonstrates pectin network without amorphous pools.